2018

3D global acceleration estimation using inertial measurement unit for biomechanical research

Revanth Raghuram Konda

ABSTRACT

3D GLOBAL ACCELERATION ESTIMATION USING INERTIAL MEASUREMENT UNIT FOR BIOMECHANICAL RESEARCH

Revanth Raghuram Konda, M.S.
Department of Mechanical Engineering
Northern Illinois University, 2018
Dr. Ji-Chul Ryu, Director

The effects of mechanical vibrations on the body of a driver in off-road vehicles such as mining vehicles have become one of the intriguing research topics. To reduce the injuries of the operator of an off-road vehicle where vibrations of high magnitude occur, an in-depth study of the nature of these vibrations must be done. The first step towards this objective is the correct estimation of acceleration of the vehicle by taking into consideration all the translational and rotational motion. The main goal of this study is the estimation of acceleration of an off-road vehicle in 3D space using an inertial measurement unit (IMU). In the past biomechanical studies, IMU along with a digital low-pass filter such as Butterworth filter has been used to estimate acceleration, but the estimation was only limited to vertical Z-direction. Also, the use of a low-pass filter requires deciding a threshold frequency by trial and error.

In this study, to obtain the best estimate of three-dimensional acceleration, an algorithm is proposed using 3D transformations, Fourier analysis, and magnitude-based filtering methods. The use of magnitude-based filtering eliminates the trial-and-error process of selecting the threshold frequency for filtering and filters out the white noise and other sources of error present in the measurement signal.

A preliminary experiment was first conducted in order to check the accuracy of the IMU used in this work. In the experiment, one-dimensional vibrations were produced in the vertical Z-direction using a heavy-duty excitor and the position was estimated using the IMU. The generated vibrations were sinusoidal with a frequency of 3Hz and a peak acceleration of 2.3 m/s^2. The estimated data using the IMU had a peak displacement of 2.38 m/s^2 with 3Hz frequency. A final experiment was conducted to verify the proposed algorithm in which a three-dimensional motion including rotation about Z-axis was generated at three different frequencies using a 6-DOF robot (Adept 850s Viper). Based on a detailed error analysis, the final experiment results indicate that the proposed algorithm produces an acceptable degree of accuracy in estimation of 3D global accelerations.

NORTHERN ILLINOIS UNIVERSITY
DE KALB, ILLINOIS

DECEMBER 2018

3D GLOBAL ACCELERATION ESTIMATION USING INERTIAL MEASUREMENT UNIT FOR BIOMECHANICAL RESEARCH

BY

REVANTH RAGHURAM KONDA

A THESIS SUBMITTED TO THE GRADUATE SCHOOL

IN PARTIAL FULFILLMENT OF THE REQUIREMENTS

FOR THE DEGREE

MASTER OF SCIENCE

DEPARTMENT OF MECHANICAL ENGINEERING

Dissertation Director:
Dr. Ji-Chul Ryu

ACKNOWLEDGEMENTS

I would like to appreciate and thank Dr. Ji-Chul Ryu, who has been providing me with abundance of knowledge, motivation and support throughout my master's program. I would like to appreciate my research group members Mr. Sandeep Reddy Erumalla, Mr. Amin Mohammadi and Mr. Maxwell Thompson for the constant help and encouragement they have provided me. I would like to thank Dr. Jenn-Terng Gau and Dr. Sachit Butail for their insightful inputs on my thesis. Last but not the least, I would like to thank the Mechanical Engineering Department for giving me this opportunity to work on this thesis.

DEDICATION

To my parents, family and friends

TABLE OF CONTENTS

Page

LIST OF TABLES vi

LIST OF FIGURES. vii

Chapter

1 INTRODUCTION 1

1.1 Motivation 1

1.2 Literature Review 2

1.3 Objective 5

1.4 Outline 5

2 INERTIAL MEASUREMENT UNIT 6

2.1 Error Characteristics and Problems in Postprocessing. 7

2.1.1 White Noise 8

2.1.2 Constant Bias. 8

2.1.3 Flicker Noise 9

3 THEORETICAL BACKGROUND AND ALGORITHM DESIGN 10

3.1 Inertial Navigation Algorithm 10

3.1.1 Orientation Estimation 11

3.1.2 Transformation of Local Data to Global Data 14

3.1.3 Simulation 15

3.2 Signal Processing 19

3.2.1 Fourier Transform. 20

Chapter Page

3.2.2 Convolution and Filtering 21

3.3 Proposed Algorithm 23

4 EXPERIMENT AND RESULTS 25

4.1 Preliminary Experiment 25

4.2 Experimental Results 29

5 CONCLUSION 35

REFERENCES 36

LIST OF TABLES

Table Page

2.1 Error Characteristics of ADIS16405 9

4.1 Repeatability 33

4.2 Error Analysis 33

LIST OF FIGURES

Figure		Page
1.1	Mining vehicle	1
2.1	ADIS16405 mounted on EVAL ADISZ evaluation board.	6
3.1	Inertial navigation algorithm.	11
3.2	Plots representing the actual and estimated values of position.	17
3.3	Plots representing the increase of error in the position estimation with time.	17
3.4	Acceleration obtained from double-differentiating estimated position..	18
3.5	Error between the estimated global acceleration and the acceleration recalculated from the estimated position.	19
3.6	Proposed algorithm.	23
4.1	Experimental setup for the preliminary experiment.	26
4.2	Acceleration in Z-direction without filter.	27
4.3	Acceleration in Z-direction obtained through the proposed algorithm.	28
4.4	Acceleration in Z-direction presented in frequency spectrum..	28
4.5	Experimental setup for the final experiment.	29
4.6	Acceleration profiles in X,Y and Z directions.	30
4.7	Comparison of reference and estimated acceleration profiles in X,Y and Z directions in time domain.	31
4.8	Comparison of reference and estimated acceleration profiles in X,Y and Z directions in frequency domain.	32

CHAPTER 1

INTRODUCTION

1.1 Motivation

The effects of mechanical vibrations on the body of a driver in off-road vehicles such as mining vehicles (Fig. 1.1) has become one of the intriguing research topics. In ordinary vehicles, the nature of vibrations is mostly in the vertical (Z-axis) direction, which can be controlled to some extent by employing vertical suspension systems. But in off-road vehicles, the combined effect of vibrations in the directions perpendicular to the Z-axis are as important as that in the vertical direction. This leads to whole-body vibration of the vehicle operator that further could lead to severe injuries and/or musculoskeletal disorders.

Figure 1.1: Mining vehicle[1].

In order to determine the effects of vibrations on the operator's body, the differences between single-axis and multi-axis vibrations need to be studied in depth. The first step

[1]http://www.npkce.com/product-categories/mining-vehicles/mining-dump-trucks/

toward this objective is the correct estimation of the global acceleration of such a vehicle. Although, a tri-axial accelerometer is typically used to capture the acceleration profile of the vibrations, it only measures linear accelerations in X, Y, and Z directions without considering rotational motion if it is present. In the off-road terrain, the vehicles are subject to angular motions that are not negligible compared to normal terrain. Under such conditions, the correct estimation of acceleration in all the three directions can be achieved by considering the angular motion. Since tri-axial accelerometers cannot capture angular motion, an inertial measurement unit (IMU) is used in which a tri-axial gyroscope is fabricated along with a tri-axial accelerometer. To simulate the vibrations of off-road vehicles, a 6-DOF Stewart platform will be used which operates with global data input. Since for the measurement of acceleration of an off-road vehicle conventional technologies such as global positioning systems (GPS) and high-quality vision systems are not suitable, in this research an IMU was used. This research will serve as a first step in finding remedies to reduce the effect of whole-body exposure to vibrations.

1.2 Literature Review

Since its origin, MEMS inertial measurement units have been used for various unconventional purposes besides navigation in different areas such as aerospace, biomechanical analysis and robotics. They are mainly used as a supporting unit for a different set of measurements taken using other technologies such as GPS or high-quality vision because IMUs estimate position using a method called dead reckoning. In dead reckoning, the process of estimating the current state of a system is only based on the previous state of the system. Even if there is a small error in one of the intermediate states, that error keeps accumulating over time and forms a larger error in the estimation of the final state. For this purpose, IMUs are not

used individually for position estimation. Decribed below are a few works in which IMU has been used as a supporting unit for other more reliable technologies. Sakib [1] demonstrated how an IMU can be implemented for increasing the accuracy of hydrographic survey in which emphasis was laid on attitude estimation of the vessel, which cannot be captured with high degree of accuracy by GPS. In robotics, IMUs are widely implemented in mobile robots and unmanned arial vehicles. Zaidner and Shapiro [2] and Wendel et al. [3] have used an IMU along with GPS for position estimation of mobile robots and UAVs respectively using sensor fusion techniques. Lou and Xin [4] used an IMU to estimate the attitude of a mobile robot by applying sensor fusion to accelrometer, gyroscope and magnetometer data. Jiang and Yin [5] used an IMU along with a vision system for robust pedestrian tracking. Ferrara et al. [6] have developed a buried object locator system by integrating ground penetrating radar (GPR) technology with GPS and IMU. For the purpose of estimating accurate location of buried objects, GPR and GPS/IMU technologies were combined such that the buried object was detected by the GPR technology and the location of the buried object was estimated by the combination of GPS and IMU. Li et al. [7] have attempted to improve the reliability and availability of GPS/INS systems by introducing range observation through ultra-wideband (UWB). An improved Kalman filter was proposed to resist the influence of gross error from UWB observation in GPS/UWB/INS tightly coupled navigation. Tian et al. [8] in their work have fused data from inertial sensors of IMU and IMU data with Kinect in order to provide robust hand position estimation. Unscented Kalman filter was employed for the purpose of sensor fusion. IMUs have also been employed for the measurement of elastic deformation. Dai et al. [9] and Lialiang et al. [10] have used IMU for this purpose.

In the past years, IMUs have been employed for biomechanical analysis. Karchnak et al. [11] in their work have employed IMU for evaluation of human biomechanical parameters by using it to evaluate the basic shoulder movements such as flexion, extension and abduction. IMU was placed on the backside of the forearm and experimental data was collected.

For accuracy purposes, the experiment was simultaneoulsy monitered by the SMART video capturing system for motion analysis. Esser et al. [12] in their work have used IMU and optical motion capture system (OMCS) to measure the center of mass position in the vertical direction and compared the results. Quaternions were used instead of roll-pitch-yaw angles to represent orientation of the person. A low-pass Butterworth filter was used to filter the transposed acceleration data before it was double integrated and compared with OMCS measurement data. Kim et al. [13] have used an IMU to measure whole-body vibrations of an agricultural tractor to improve multi-axial suspension systems. Both linear accelerations and angular accelerations were recorded to get a more realistic simulation. Noise was filtered out from the accelerometer and gyroscope data using Fourier analysis and low-pass filter to get practical position values which were within the limits of a 6-DOF motion platform that was used to simulate the whole-body vibrations in an indoor environment. IMUs have found applications in the sports industry and wearable portable devices for biomechanical analysis. The use of IMU with GPS over object tracking systems for position estimation has an advantage in terms of the operating space. Zihajehzadeh et al. [14] have used IMU along with GPS to estimate position for the purpose of gauging the overall performance of an athlete. The IMU was mounted onto the body of the athlete using a wearable portable device. Extended Kalman filter was used for data fusion to achieve higher accuracy over a linear Kalman filter. Schmidt et al. [15] have also used IMU for similar purposes in their work. IMU was used for field-based performance analysis through an accurate detection of step parameters in sprinting.

As can be noticed from the above-mentioned works, IMUs are mainly used as a supporting system for another measuring unit such as GPS or vision system along with Kalman filter when it comes to position measurement. IMU cannot be used individually for estimating position using Kalman filter from the acceleration data as the mathematical model describing the functioning of an IMU was found to be unobservable (see [16] for the definition of

unobservability). Hence only global acceleration with minimum error can be obtained using an IMU. Traditional signal-processing tools can be used to filter the signals from an IMU but the accuracy of acceleration calculation will be compromised to some extent because of the complexity of the algorithm [17] being used to calculate it from the accelerometer and gyroscope readings.

1.3 Objective

The main goal of this research is to accurately estimate global accelerations of an off-road vehicle to study the effects of whole-body vibrations on the driver. Due to the limitations of an IMU regarding position estimation which was explained above, the scope of this study is limited to correct estimation of global acceleration using an IMU. Since both the sensor readings contain different sources of error, the process of combining the data becomes complex. In order to deal with this problem, two engineering tools will be used: coordinate frame transformations and digital signal processing.

1.4 Outline

The rest of this thesis is organized as follows. The in-depth details of an inertial measurement unit including error characteristics are discussed in Chapter 2. The explanation of the background theory for the proposed algorithm, inertial navigation algorithm and digital signal processing are presented in Chapter 3. The experiments performed to verify the proposed algorithm and the results are discussed in Chapter 4, followed by concluding remarks in Chapter 5.

CHAPTER 2

INERTIAL MEASUREMENT UNIT

Inertial navigation is a self-contained navigation technique in which the position and orientation of a body is calculated without utilizing any external medium such as satellites, provided that the initial position, velocity and orientation of the object are known. This technique is commonly known as dead reckoning. Because of this dead reckoning, IMU is typically used with another object tracking technology, such as global positioning system or vision system, to minimize the effect of dead reckong on the estimated data. Fig. 2.1 shows the IMU which was used in this work.

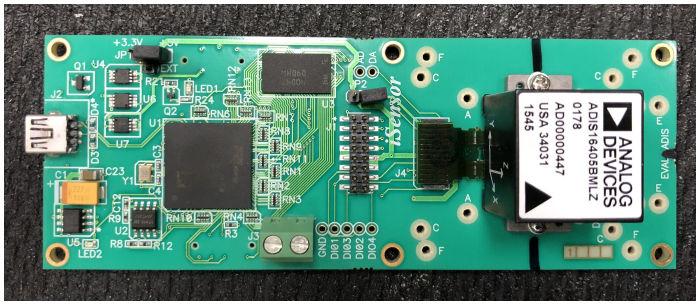

Figure 2.1: ADIS16405 mounted on EVAL ADISZ evaluation board.

An IMU typically consists of a 3-axis accelerometer, which gives the acceleration of the object, and a 3-axis gyroscope, which gives the angular velocity of the object [17]. A more sophisticated IMU utilizes a 3-axis magnetometer along with a gyroscope to measure rotations with higher degree of accuracy. By processing the signals obtained from these sensors, the position and orientation of an object can be estimated. Inertial measurement units have a wide range of applications in various fields. Among them are navigation of aircrafts, guided missiles, submarines and ships. Recent advances in MEMS technology

have enabled the fabrication of light-weight, compact inertial measurement units allowing researchers to capture the motion of human beings and animals. The IMU (Analog Devices ADIS16405) used in this thesis consists of a 3-axis accelerometer, a 3-axis gyroscope and a 3-axis magnetometer. A companion board (EVAL ADISZ) can be used for easier processing of data. A specific software package (IMU Evaluation) also provided by analog devices is used to record the output data of the module. This module is mainly designed for postprocessing purposes and is not for real-time applications. The maximum sampling rate at which the module operates is 819.2 samples per second [18], with lower sampling rates available.

2.1 Error Characteristics and Problems in Postprocessing

The drawback of using an IMU is that it utilizes dead reckoning for the estimation of position and orientation. Dead reckoning is a process of calculating current position of a system using its previous position. A small error in the previous position propagates throughout the estimation, which would cause erroneous end result. Hence, in order to minimize this error, the error in the measurements taken by an IMU along with the approximation errors in the calculations have to be minimized. Various types of noises due to calibration errors, offset in orientation and temperature effects are present in the output signal of an IMU. The three main noises which show significant effect on the output of the IMU when subjected to postprocessing are listed below:

1. White noise
2. Constant bias
3. Flicker noise

2.1.1 White Noise

White noise is a set of serially uncorrelated random numbers with zero mean and a finite variance. White noise is present in almost all sensor data in general and in most cases can be eliminated using traditional filtering methods such as low-pass filtering. For IMUs, a thermo-mechanical noise is present, which fluctuates continuously at a rate much higher than the sampling rate of the sensors. This noise can be modelled as white noise. Post-processing of IMU output data involves subjecting the data to double integration. Double integrating white noise would lead to accumulation of error over time and causes something known as random walk. The manufacturer mentions the effect of this random walk on the output with respect to time. This information can be used to minimize the effect of white noise on the position estimates to a certain extent.

2.1.2 Constant Bias

Bias is nothing but the difference between the actual value and the sensor value when the sensor is not subjected to any kind of change. Both the accelerometers and gyroscopes in the IMU have a small offset or bias which accumulates over time when subjected to integration. This can be removed by simply subtracting the offset value from the sensor readings. Removing offset or bias is very critical, as it exhibits maximum effect on the output.

2.1.3 Flicker Noise

The bias of the sensor wanders randomly over time due to flicker noise. The effects of flicker noise are generally observed when the IMU is being operated at low frequencies. At high frequencies, the flicker noise is over-shadowed by white noise. Flicker noise also causes random walk, the effect of which is specified with respect to time by the manufacturer.

Table 2.1 shows the specifications of the gyroscope and the accelerometer modules, which denote the effects of the above-described noises on the output with respect to time. More detailed explanations on the terms mentioned in the table is available in [17].

Table 2.1: Error Characteristics of ADIS16405

PARAMETERS	**COMMENTS**	**TYPICAL VALUE**	**UNITS**
GYROSCOPE			
Initial Bias	1σ	3	$^\circ$/sec
In-run Bias Stability	1σ	0.007	$^\circ$/sec
Angular Random Walk	1σ	2.0	$^\circ/\sqrt{hr}$
ACCELEROMETER			
Initial Bias	1σ	50	mg
In-run Bias Stability	1σ	0.2	mg
Random Walk	1σ	0.2	m/sec/$\sqrt{hr}$

The integration of white noise and bias instability result in the first-order and the second-order random walk. The variance with which these random walks grow is given by the typical values for in-run bias stability and random walk mentioned in the table. The typical value for initial bias is also mentioned in the table.

CHAPTER 3

THEORETICAL BACKGROUND AND ALGORITHM DESIGN

3.1 Inertial Navigation Algorithm

The output of the IMU represents the acceleration of an object with respect to its own coordinate frame attached to the body (the body frame hereafter). These acceleration readings must be accurately transformed to the global coordinate frame in order to be properly used in biomechanical studies such as operating a Stewart motion platform. For this purpose, the gyroscope readings are utilized. Using the gyroscope readings, a rotation matrix, which defines an orientation between two different coordinate frames [19], is constructed at every time step and is used to transform the raw IMU data expressed in the body frame to the global frame. Numerical double integration can then be used for position estimation. The inertial navigation algorithm (INA) is typically used to estimate position. For this reason the INA will be explained from a position estimation point of view in this section. However, in this thesis, since global acceleration estimation is critical, the utilization of INA will be focused on global acceleration estimation. The procedure above is summarized in the following steps:

1. Collect the raw data.
2. For each time step, construct a transformation matrix.
3. Using the transformation matrix, convert the local values to global values.
4. Perform a double integration on the converted global data.

Fig. 3.1 shows these steps graphically.

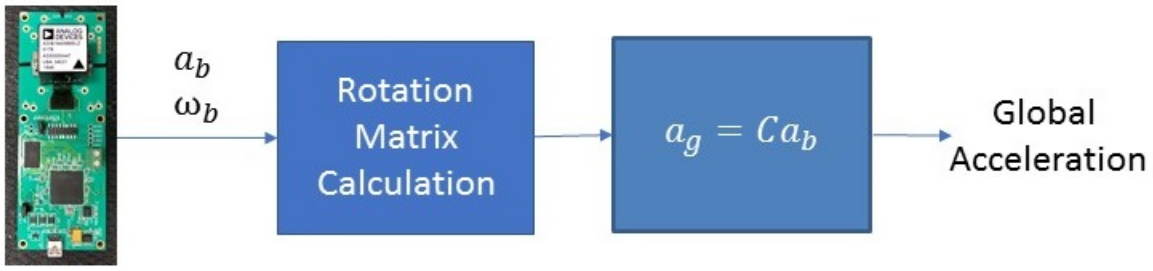

Figure 3.1: Inertial navigation algorithm.

While the basic theory for the suggested method is available in [17], we present it here since it is central to understand the proposed algorithm. As mentioned earlier, the IMU outputs the acceleration and angular velocity of a body in its local frame, not in the global frame. Therefore the raw acceleration data cannot be simply double integrated to estimate position. The acceleration data has to be first transformed from the local frame to the global frame before integration. For this purpose, rotation matrix is needed, which can be constructed using the angular velocity data from the gyroscope. The construction of the rotation matrix is a vital step in the algorithm, as any errors in this step would lead to an inaccurate transformation of the acceleration data. The theoretical backgrounds of the proposed algorithm are separately explained in detail below.

3.1.1 Orientation Estimation

The rotation matrix is used to provide a relation between the representations of a vector in two different reference frames. By assuming small angle approximation, it can be constructed by numerically integrating the angular velocities obtained as gyroscope readings.

The constructed rotation matrix can then be used for coordinate transformation of a vector such that

$$v_g = Cv_b$$

where v_g is the representation of a vector v in the global frame, v_b is the representation of v in the body frame and C is the rotation matrix. Numerical integration of angular velocity does not always lead to orientation. This applies only for infinitesimally small rotations, as it will be shown below. To estimate the orientation at a given time, simultaneous transformations have to be performed. The rotation matrix has to be tracked through time. The rate of change of the rotation matrix C is given by

$$\dot{C}(t) = \lim_{\delta t \to 0} \frac{C(t + \delta t) - C(t)}{\delta t} \tag{3.1}$$

and $C(t + \delta t)$ can be written as a product of two matrices as follows:

$$C(t + \delta t) = C(t)A(t)) \tag{3.2}$$

where $A(t)$ is the rotation matrix that relates the body frame at time t to the body frame at time $t + \delta t$. Let $\delta\phi$, $\delta\theta$ and $\delta\psi$ be the small rotations by which the body is rotated about X, Y and Z axes respectively. Using the small angle approximation, A can be written as follows:

$$A(t) = I + \delta\tau$$

where

$$\delta\tau = \begin{bmatrix} 0 & -\delta\psi & \delta\theta \\ \delta\psi & 0 & -\delta\phi \\ -\delta\theta & \delta\phi & 0 \end{bmatrix}$$

Substituting $C(t+\delta t)$ in Eqs. (3.1) and (3.2), we obtain

$$\dot{C} = C(t) \lim_{\delta t \to 0} \frac{\partial \tau}{\partial t}$$

using the small angle approximation

$$\lim_{\delta t \to 0} \frac{\partial \tau}{\partial t} = \Omega(t)$$

where

$$\Omega(t) = \begin{bmatrix} 0 & -\omega_{bz}(t) & \omega_{by}(t) \\ \omega_{bz}(t) & 0 & -\omega_{bx}(t) \\ -\omega_{by}(t) & \omega_{bx}(t) & 0 \end{bmatrix}$$

Here Ω_{bx}, Ω_{by}, and Ω_{bz} are the angular velocities about each axis of the local frame. Hence, the rotation matrix can be obtained by solving the following differential equation:

$$\dot{C}(t) = C(t)\Omega(t) \tag{3.3}$$

The solution of the above equation is given by

$$C(t) = C(0) \exp(\int_0^t \Omega(t)dt) \tag{3.4}$$

where $C(0)$ is the initial orientation of the body. Practically, the IMU outputs data at a fixed time interval. Hence the above equation can be modified as follows:

$$C(t) = C(t) \exp(\int_t^{t+\delta t} \Omega(t)dt)$$

By applying the rectangular rule for numerical integration

$$\int_{t}^{t+\delta t} \Omega(t)dt = B = \begin{bmatrix} 0 & -\omega_{bz}(t) & \omega_{by}(t) \\ \omega_{bz}(t) & 0 & -\omega_{bx}(t) \\ -\omega_{by}(t) & \omega_{bx}(t) & 0 \end{bmatrix} \delta t$$

with $\omega_b = (\omega_{bx}, \omega_{by}, \omega_{bz})^T$ and $\sigma = |\omega_b|\delta t$ and by performing Taylor expansion of the exponential term, the rotation matrix at a discrete time can be written as

$$C(t+\delta t) = C(t)(I + \frac{\sin\sigma}{\sigma}B + \frac{1-\cos\sigma}{\sigma^2}B^2)$$

3.1.2 Transformation of Local Data to Global Data

Once the rotation matrix is obtained, the next step is to transform the local acceleration data to global acceleration data using this rotation matrix. Then double integration of the transformed acceleration data gives the global position data. Assuming the acceleration signal obtained from the IMU to be $a_b(t) = [a_{bx}(t), a_{by}(t), a_{bz}(t)]^T$, these operations can be done using the following equations at a time t:

$$a_g(t) = C(t)a_b(t) \tag{3.5}$$

$$v_g(t+\delta t) = v_g(t) + a_g(t)\delta t$$

$$s_g(t+\delta t) = s_g(t) + v_g(t)\delta t + \frac{1}{2}a_g\delta t^2$$

where v_g is the global velocity and s_g is the global position of the body.

3.1.3 Simulation

In order to verify the correct implementation of the algorithm explained in the previous section, a simulation was conducted. For this purpose, artificial global accelerations and orientations with respect to each global axis were first chosen as a function of time. Using these global accelerations and orientation, corresponding artificial local accelerometer and gyroscope data were computed at given times, which represent raw IMU readings at a selected sampling rate. Then the position was estimated using the method described in the previous section as if it were done using actual IMU data. Finally, the estimated position was compared with the actual position that can be precisely calculated using the artificial global accelerations and orientations we defined in the beginning. The sampling rate selected was 1 kHz. In the numerical implementation of the integration algorithm, the rectangular integration method was employed. The units of the estimated position are meters. The artificial values for the global acceleration (m/s^2) and orientation (rad) chosen as a function of time are

$$a_{gx}(t) = 2t + 3$$

$$a_{gy}(t) = 3t + 4$$

$$a_{gz}(t) = 4t + 5$$

Orientations α, β, γ with respect to X, Y and Z axes, respectively:

$$\alpha = 3\cos(t + \pi/3)$$

$$\beta = 2\cos(t + \pi/5)$$

$$\gamma = \cos(t)$$

where the global acceleration $a_g = [a_{gx}, a_{gy}, a_{gz}]^T$. Let R_x, R_y and R_z be the rotation matrices when the object under consideration is rotated by an angle α, β, γ about the global (fixed) X, Y and Z axes respectively. Then the rotation matrix C can be obtained as follows [19]:

$$C = R_z R_y R_x$$

where, with the shorthand notation $c_\theta = \cos(\theta)$ and $s_\theta = \sin(\theta)$,

$$R_x = \begin{bmatrix} 1 & 0 & 0 \\ 0 & c_\alpha & -s_\alpha \\ 0 & s_\alpha & c_\alpha \end{bmatrix}, R_y = \begin{bmatrix} c_\beta & 0 & s_\beta \\ 0 & 1 & 0 \\ -s_\beta & 0 & c_\beta \end{bmatrix}, R_z = \begin{bmatrix} c_\gamma & -s_\gamma & 0 \\ s_\gamma & c_\gamma & 0 \\ 0 & 0 & 1 \end{bmatrix}$$

Using this rotation matrix with the predefined global acceleration and orientation, the local angular velocities are derived using Eq. (3.3) as follows:

$$\Omega(t) = C(t)^T \dot{C}(t)$$

Also, the local accelerations are obtained using Eq. (3.5).

$$a_b(t) = C(t)^T a_g(t)$$

Fig. 3.2 shows the actual and estimated positions. Fig. 3.3 shows the error of the estimated values from the actual ones.

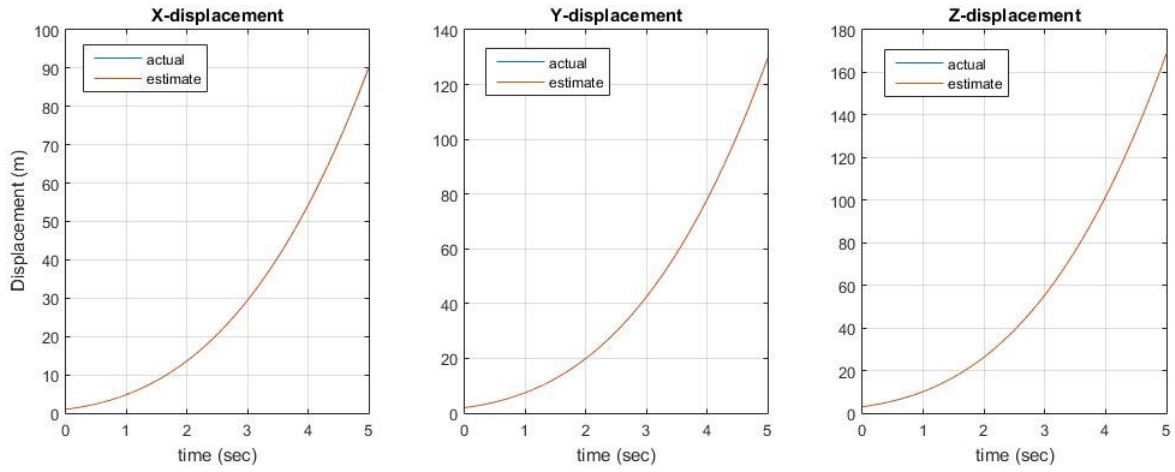

Figure 3.2: Plots representing the actual and estimated values of position.

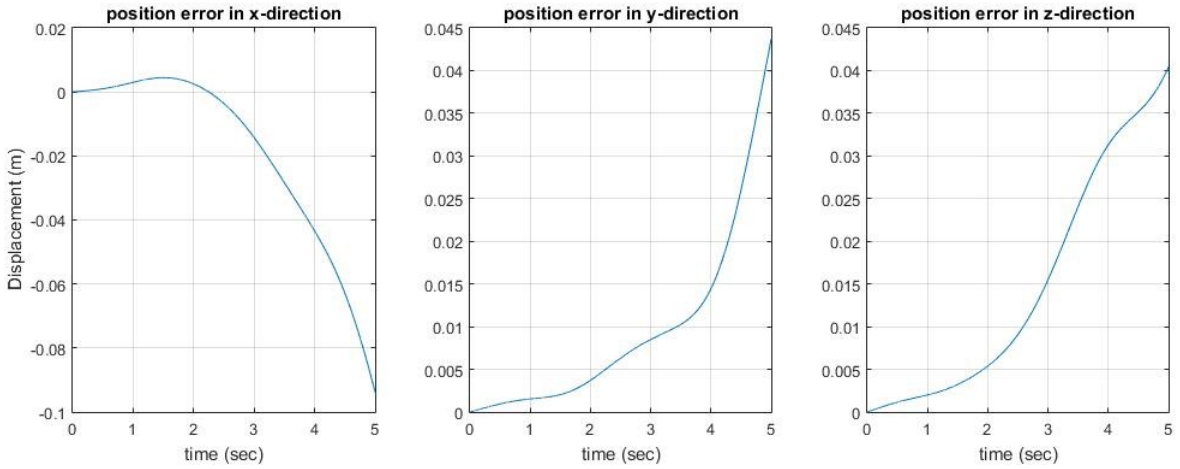

Figure 3.3: Plots representing the increase of error in the position estimation with time.

As shown, the error between the actual and estimated values increases over time, which results from numerical integration and the small angle approximation considered in the rotation matrix construction. This type of error in estimation is unavoidable since the numerical integration and constructing rotation matrix using the small angle approximation are required for position estimation as explained in the previous section. We do not show the results here, but it is clear that the error will be reduced with a higher sampling rate.

An effort was made to obtain acceleration from the estimated position using numerical differentiation, and this acceleration was compared with the original acceleration. The purpose of this work is to observe the effect of the error in position estimation on acceleration generated using the estimated position. This is the case when a vibration simulator would take (estimated) position input while generated acceleration is of more interest. Fig. 3.4 shows the recalculated acceleration obtained from numerically differentiating the estimated position (shown in Fig. 3.2) with respect to the same sampling time.

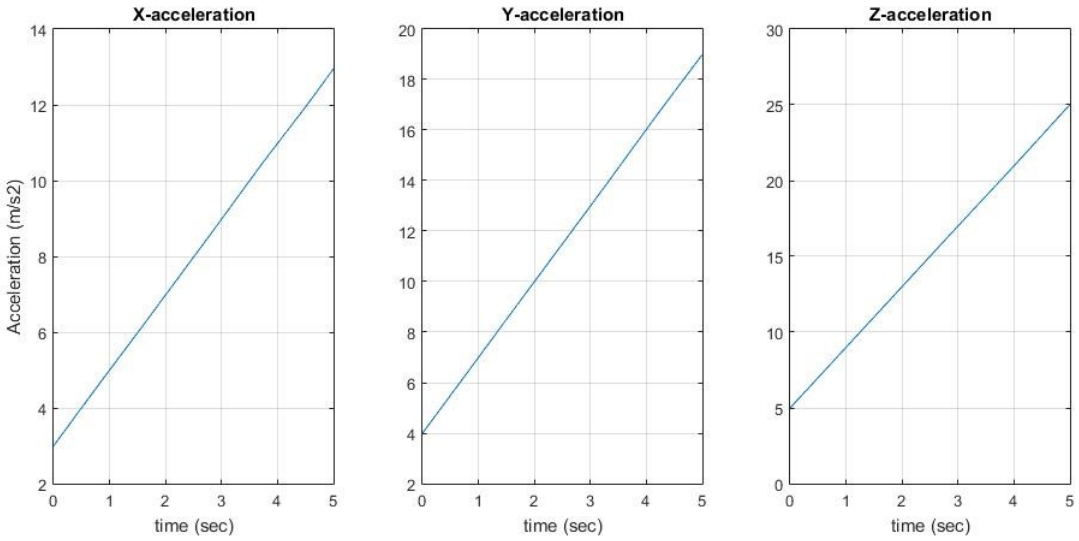

Figure 3.4: Acceleration obtained from double-differentiating estimated position.

The error between the estimated global acceleration and the acceleration recalculated from the estimated position is shown in Fig. 3.5. It should be noted that we compare the recalculated acceleration with the estimated, not the actual, global acceleration. That is because in practice the actual global acceleration would not be available unlike this simulation.

As shown in Fig. 3.5 , the difference between the two compared variables is practically zero. In fact, it is easily expected because they are simply numerical double integration and numerical double differentiation with the same amount of time interval δt. For this reason, no noticeable error between the estimated global acceleration and the acceleration

recalculated from the estimated position would be obtained even with the simulation data with noise or experimental data. Hence, it can be concluded that obtaining a better estimate of global acceleration from body acceleration is much more critical.

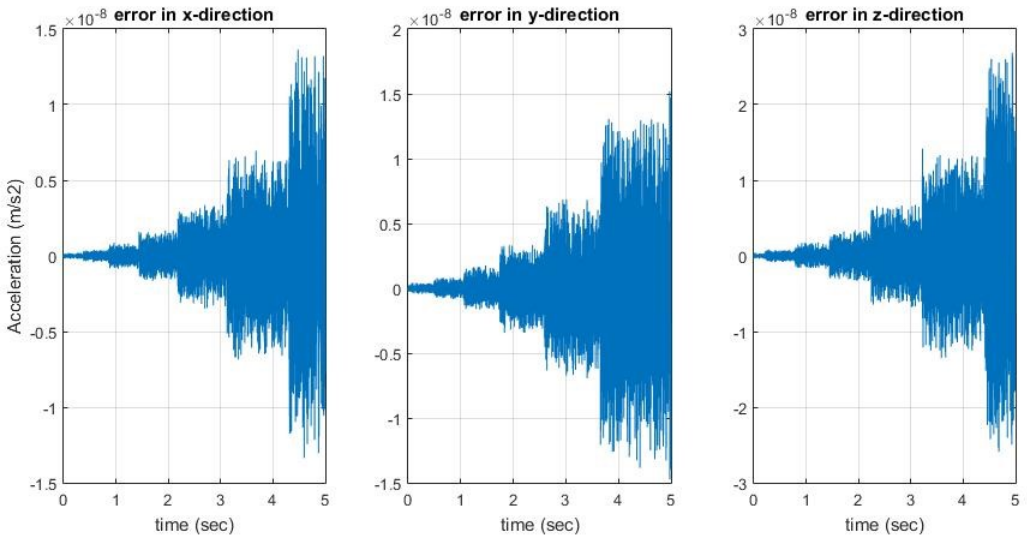

Figure 3.5: Error between the estimated global acceleration and the acceleration recalculated from the estimated position.

3.2 Signal Processing

All the physical quantities in the real world are continuous or analog signals. However, the process of measuring sensor data should be dealt with in a discrete or digital fashion. In addition, the actual measured values are influenced by the imperfections of the measuring device or the sensor. For these reasons, some important characteristics of the measured signal could be masked. To extract the necessary information from the measured signal, certain mathematical operations have to be performed. Signal processing is a process of modifying a given signal to eliminate noise and other interferences to obtain the desired characteristics from it. Sometimes, handling the data in frequency domain is desirable.

Based on the application, frequency terms that are related to unwanted values are eliminated. The frequency content of a given signal is obtained through Fourier transform and the removal of unwanted frequencies is done by a mathematical operation called convolution. Although these two concepts are well known, they are explained below since they are crucial to understand the proposed algorithm in section 3.3.

3.2.1 Fourier Transform

Fourier transform is one of the major mathematical tools which comes under a broader area of study known as the Fourier analysis. The other mathematical tool of the Fourier analysis is the Fourier series. Fourier analysis is mainly used to represent any given signal (defined in time domain) in the frequency domain. For periodic functions, Fourier series is used, and for signals with finite energy, Fourier transform is used. In this thesis Fourier transform is used, as signals with finite energy are being dealt with. The main aim of Fourier analysis is to represent any given signal in terms of scaled sinusoidal waves, which in turn define the frequency content of the signal. For non-periodic signals this can be achieved by the Fourier transform. The Fourier transform of a given signal is defined as follows [20]:

$$F[f](\omega) = \int_{-\infty}^{\infty} f(t)e^{-i\omega t}dt$$

where ω is the frequency. For mathematical convenience, to define negative frequencies harmonically related complex exponentials are used [21]. Since in the present work digital or discrete signals are being dealt with, discrete Fourier transform (DFT) has to be employed.

The discrete Fourier transform of a given signal u described by N discete data points is defined as follows [20]:

$$D[u](k) = \sum_{j=0}^{N-1} u_j e^{-2\pi ijk/N}$$

where D is the DFT operator and k is the frequency in discrete format. Using these mathematical tools, the frequency content of a given signal can be studied and can be further used to extract important information using filtering methods, which will be explained in the next section.

3.2.2 Convolution and Filtering

Convolution is a mathematical operation which takes in two functions as an input to produce a new function. In mathematical terms it is defined by the following equation [20]:

$$f * g = \int_{-\infty}^{\infty} f(t-\tau)g(\tau)d\tau$$

where $f(t)$ and $g(t)$ are two functions of time and τ is a dummy variable used to perform the integration. The symbol $*$ is used to define the convolution operation. The Fourier transform has an interesting property known as the convolution property. The property states that the convolution of two functions in the time domain is equivalent to the product of them in the frequency domain, i.e.,

$$(f * g)(t) \leftrightarrow F(\omega)G(\omega)$$

A more detailed proof of this property is explained in [22]. This property forms the basis for digital filter design. Using this property, any given signal can be altered or modified to extract useful information.

As stated earlier, through Fourier analysis a given signal can be decomposed into the sum of infinite scaled sinusoidal terms of different fequencies. The frequencies of the sinusoidal waves represent the frequency content of the signal and the scaled values represent the amplitude or magnitude of the sinusoidal terms. In filtering, the signal is modified such that it is a linear combination of only a handful of sinusoidal terms, not all the infinite terms which actually represent it. The filter is always designed in frequency domain based on either frequency or magnitude because it is mathematically convenient. Typically in frequency-based filtering sinusoidal signals with frequencies less than a certain threshold frequency, only is considered for the linear combination and the rest are eliminated. This type of filter is called a low-pass filter. Mathematically it can be written as [20]

$$f_o(\omega) = \begin{cases} f(\omega) & \text{for } \omega \leq \omega_o \\ 0 & \text{for all other conditions} \end{cases} \tag{3.6}$$

where f_o is the filtered signal in frequency domain, f is the actual signal in frequency domain and ω_o is the threshold frequnecy. On the contrary, in a high-pass filter, signals with frequencies higher than the threshold frequency will only be considered. The other kind of filter is a band-pass filter, which only passes signals with frequencies in a certain range. This type of filtering has one shortcoming, called Gibbs phenomenon [20]. This appears when the filtered signal is transformed into time domain through inverse Fourier transform. There are filter designs that tackle this problem but they are beyond the scope of this thesis [22].

The other type of filtering is based on magnitude, where similar to frequency-based filtering, signals with magnitude greater than a certain threshold magnitude are considered and the other signals are eliminated. This can be written mathematically as

$$f_o(\omega) = \begin{cases} f(\omega) & \text{for } f(\omega) \geq A \\ 0 & \text{for all other conditions} \end{cases} \tag{3.7}$$

where f_o is the filtered signal in frequency domain, f is the actual signal and A is the threshold magnitude.

3.3 Proposed Algorithm

As discussed in Chapter 1, IMUs are typically used as a supporting unit to improve the displacement estimates or acceleration estimates from another source of measurement. In this thesis, however, the IMU is being used individually to capture the acceleration profile of vibrations. In order to accurately capture the vibrational characteristics of the motion, the raw data collected by the IMU has to be processed before the inertial navigation algorithm is applied. The algorithm proposed in this thesis takes in the raw IMU data and filters out the unwanted characteristics such as noise and linearity in the signals and passes them onto the inertial navigation algorithm, which transforms local acceleration to global acceleration. Fig. 3.6 shows the sequence of operations performed by the proposed algorithm.

Figure 3.6: Proposed algorithm.

Among the two types of filters, frequency-based filter and magnitude-based filter, in this work magnitude-based filter is used. The threshold magnitude for the filter is calculated such that signals with considerably lower magnitudes than the other signals are removed from the data. This is achieved by calculating the average of magnitudes of all the signals and multiplying the average by a scale factor. The algorithm is designed such that it minimizes the various sources of error such as bias, bias instability and white noise. By also removing the zero-frequency term, it eliminates the linearity in the output signals and only captures the profiles related to vibrations that can be used for further biomechanical analysis. Using this proposed algorithm, the global acceleration values of an off-road vehicle in all the three X, Y, and Z directions can be estimated. The proposed algorithm can be summarized by algorithm 1:

Algorithm 1: Proposed algorithm

Input : Raw IMU data (Accelerometer and Gyroscope readings)
Output: Global acceleration in X,Y,Z directions

FILTER:
for *Each signal* **do**
  $f(\omega = 0) = 0$;
  Calculate threshold magnitude;
  if $f(\omega) < ThresholdMagnitude$ **then**
    $f(\omega) = 0$;
  else
    $f(\omega) = f(\omega)$;
  end
end
TRANSFOMATION:
for *Each timestep: Using filtered signals* **do**
  Calculate rotation matrix: $B = \begin{bmatrix} 0 & -\omega_{bz}(t) & \omega_{by}(t) \\ \omega_{bz}(t) & 0 & -\omega_{bx}(t) \\ -\omega_{by}(t) & \omega_{bx}(t) & 0 \end{bmatrix} \delta t$
  $\omega_b = (\omega_{bx}, \omega_{by}, \omega_{bz})^T$; $\sigma = |\omega_b|\delta t$ $C(t + \delta t) = C(t)(I + \frac{\sin\sigma}{\sigma}B + \frac{1-\cos\sigma}{\sigma^2}B^2)$;
  Transform data from local frame to global frame: $a_g(t) = C(t)a_b(t)$
end

CHAPTER 4

EXPERIMENT AND RESULTS

The verification of the proposed algorithm was achieved through two experiments. In the preliminary experiment, the accuracy of the combined pair of the IMU and the proposed algorithm under no rotation condition was verified, and in the final experiment the performance of the algorithm under rotation was studied.

4.1 Preliminary Experiment

As mentioned above, the main purpose of the preliminary experiment is to verify the accuracy of the IMU in combination with the proposed algorithm under no rotation condition. Fig. 4.1 shows the experimental setup of the preliminary experiment. The experimental setup consists of a heavy-duty excitor (used to generate a periodic motion), a well-calibrated uni-axial accelerometer, whose measurements are considered as the reference for the experiment, and the IMU placed on the top of the excitor.

The excitor was set up such that it generates a sinusiodal motion in the vertical Z-direction with a peak acceleration of 2.3 m/s^2 at a frequency of 3 Hz. Since the purpose of this experiment was to only verify the accuracy of the algorithm under no rotation condition, the periodic motion was generated only in the vertical direction. The sampling frequency of the IMU was set to be 409.601 samples per second. The data was collected for 12 seconds during the experiment. Fig. 4.2 shows the estimated acceleration in Z-direction using the inertial navigation algorithm (INA) without the application of the digital filtering.

Figure 4.1: Experimental setup for the preliminary experiment.

As it is clearly seen, although the sinusiodal characteristic of the motion was captured by the INA, there is a continuous increase in the profile which arises due to the numerical integration of noisy and biased angular velocity readings as discussed in Chapter 2. Fig. 4.3 shows the obtained estimates for acceleration in Z-direction using the proposed algorithm, i.e., when the raw IMU data is filtered using the proposed magnitude-based filter and then passed to the inertial navigation algorithm.

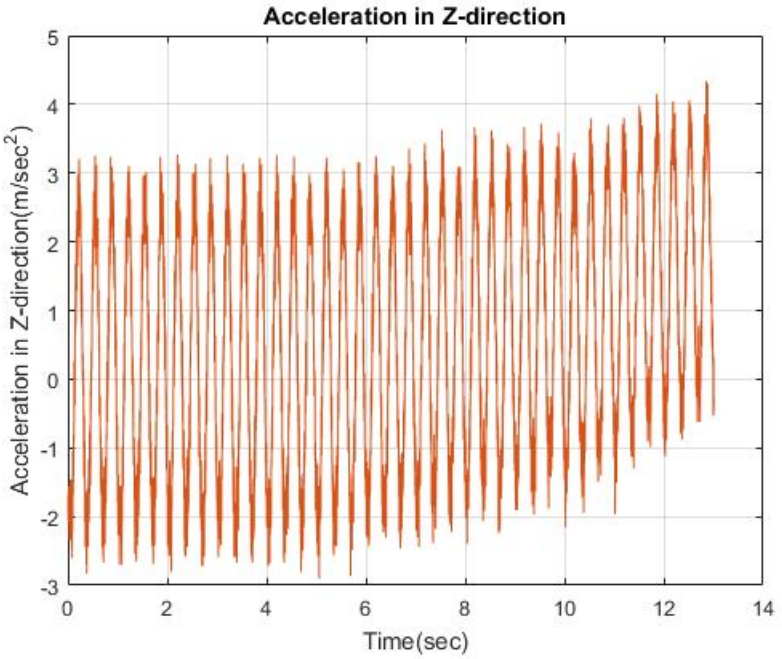

Figure 4.2: Acceleration in Z-direction without filter.

As can be noticed from the figure, the continously increasing nature observed in the previous case as well as the overall noise is eliminated. As shown in Fig. 4.4 the obtained signal has a frequency of 3Hz and a peak acceleration value of 2.38 m/s^2 giving an error of 0.08 m/s^2 from the reference signal. Therefore, we conclude that the IMU in combination with the proposed algorithm estimates the global acceleration with an acceptable amount of accuracy under no rotation condition.

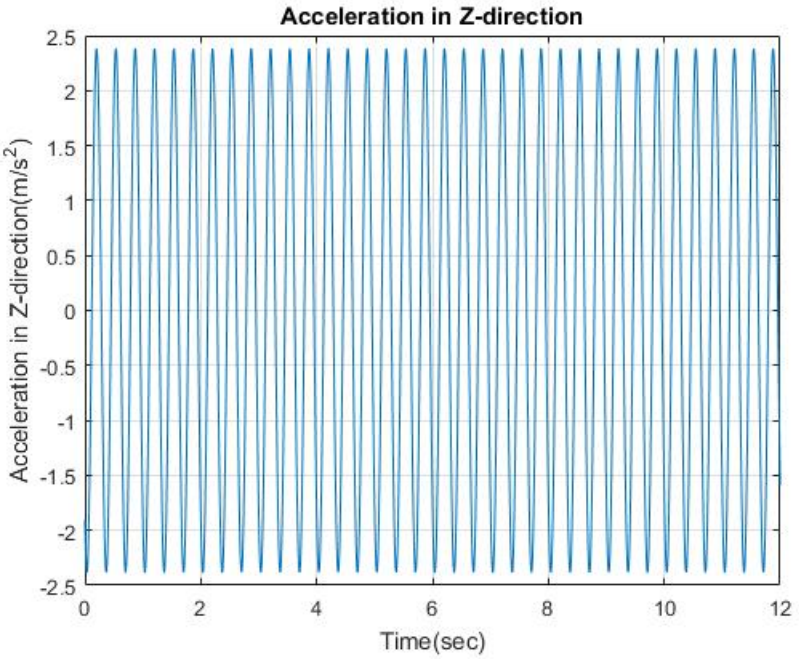

Figure 4.3: Acceleration in Z-direction obtained through the proposed algorithm.

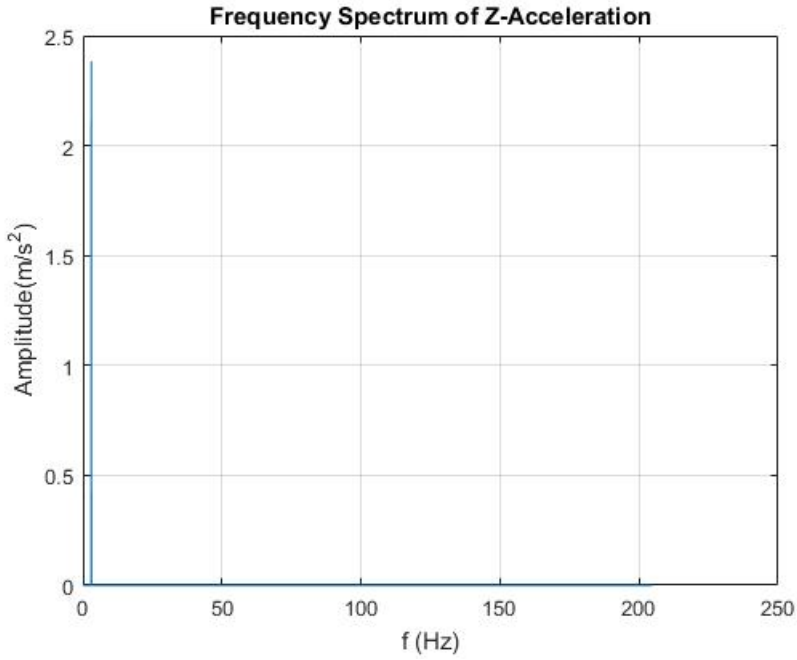

Figure 4.4: Acceleration in Z-direction presented in frequency spectrum.

4.2 Experimental Results

In this section, we present experimental results showing the performance of the proposed algorithm under rotation condition. In order to generate a three-dimensional motion with rotation, Adept 850s Viper robot was used. Fig. 4.5 shows the experimental setup.

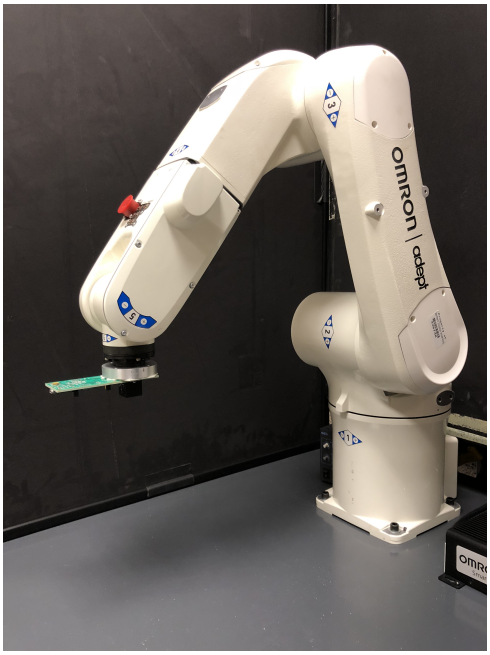

Figure 4.5: Experimental setup for the final experiment.

The IMU is mounted on the end effector of the robot such that the Z-axis of the IMU is aligned with the rotational axis of the end effector. Due to the limitations of the robot functionalities, the position of the end effector could not be recorded continuously between short time intervals, which meant that there was no reference data to check the performance of the algorithm. In order to overcome this drawback, an experiment was conducted in which the end effector moved in a periodic motion in all three X, Y, and Z directions simultaneously without any rotations. Then, using the IMU, the acceleration data was collected. With the

proven accuracy from the preliminary experiment, the data collected were used as a reference for the final experiment.

A periodic motion was generated using the robot such that the end effector moves through a distance of 9 cm in all three directions with a frequency of 2.3 cycles per second. The same motions of experiment were conducted three times to check the repeatability of the motion generated by the robot. Fig 4.6 shows the results of the three experiments.

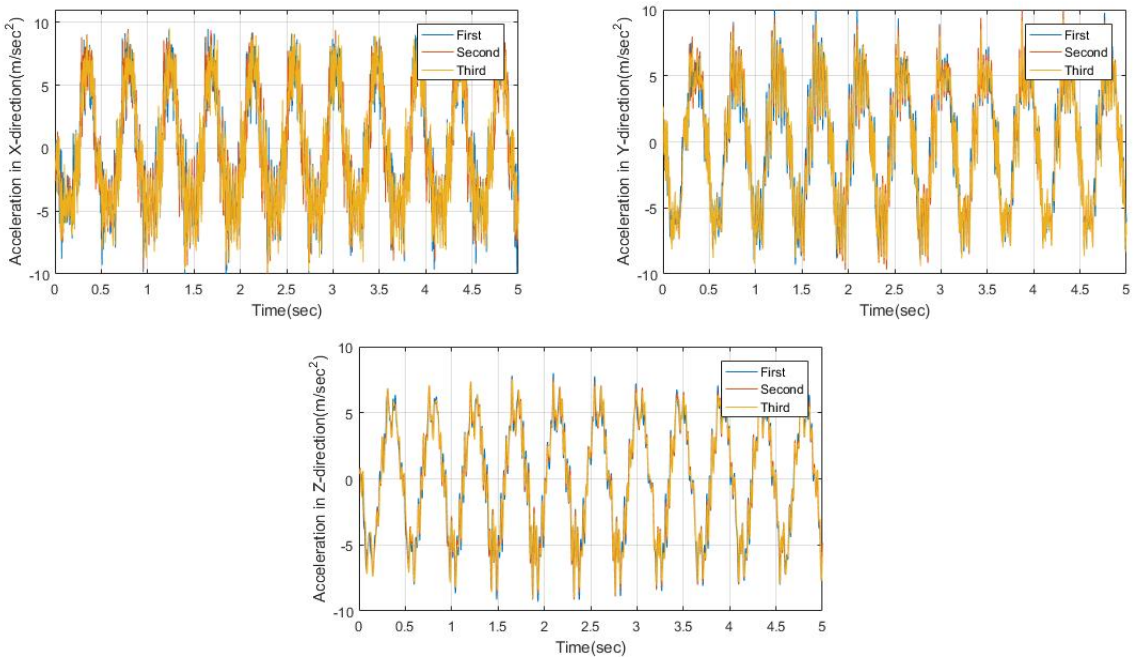

Figure 4.6: Acceleration profiles in X,Y and Z directions.

The figures show that the profiles obtained from the three experiments are very close, as the repeatability for this particular motion was calculated to be 1.42 m/s^2, 0.78 m/s^2, 0.38 m/s^2 in X, Y and Z directions respectively. At each time step, for each axis, the standard deviation of global acceleration values obtained from the three trials was calculated. Then the obtained standard deviations were averaged to obtain the repeatability. The reference data was determined by calculating the average of the three data sets. The peak values of the reference are 5.87 m/s^2, 6.04 m/s^2 and 5.83 m/s^2 in X, Y, and Z directions respectively.

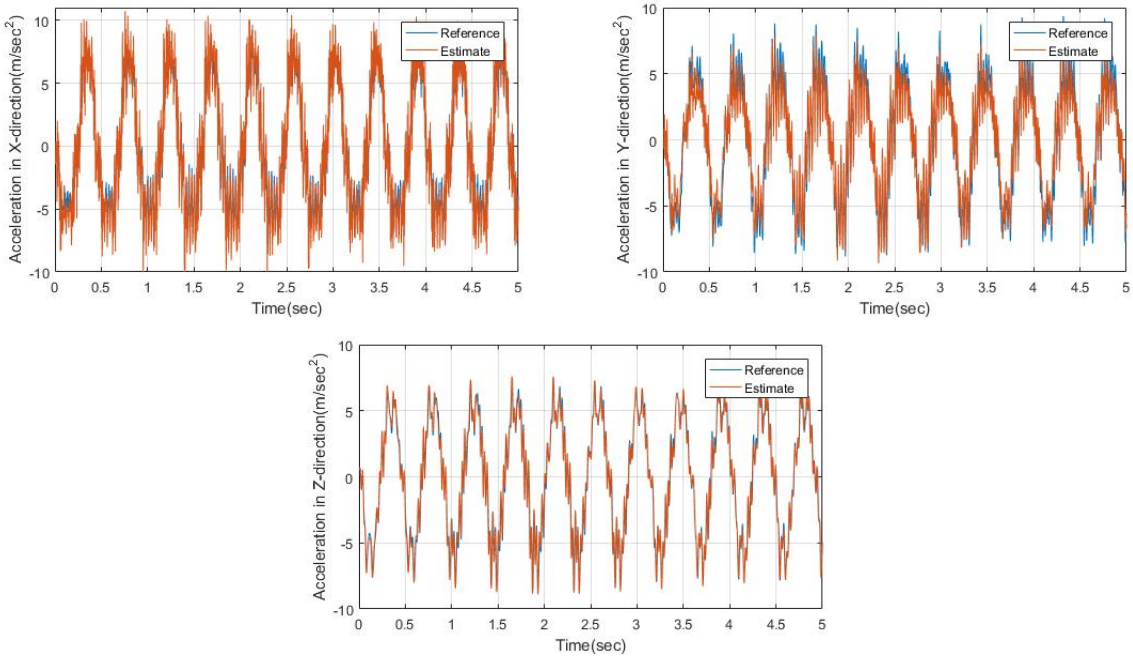

Figure 4.7: Comparison of reference and estimated acceleration profiles in X,Y and Z directions in time domain.

For the final experiment, on top of the same translational motion described above, a rotation about Z-axis was added. The end effector moved through an angular displacement of 25° while simultaneously moving through a distance of 9 cm in X, Y and Z directions. The frequency of this motion was 2.3 cycles per second. Since the global accelerations of the end effector in the both cases are the same, the acceleration estimates through the proposed algorithm can be compared with the no rotation case as a reference. Fig. 4.7 shows a comparison between the profiles of the reference and estimated accelerations in time domain.

As can be seen, the algorithm performs satisfactorily in estimating the accelerations in terms of peak accelerations and frequency components when compared to the reference estimates. The peak accelerations of the data obtained from the experiment are 6.62 m/s^2, 4.73 m/s^2 and 5.84 m/s^2 in X, Y, and Z directions respectively. The RMS error in the

three directions was found to be 1.67 m/s^2, 1.19 m/s^2, and 0.42 m/s^2. The periodicity and the overall profile are captured but there is a minor error in the peak values between the estimates and the reference data. Fig. 4.8 shows a comparison between the profiles of the reference and estimated acceleration in frequency domain.

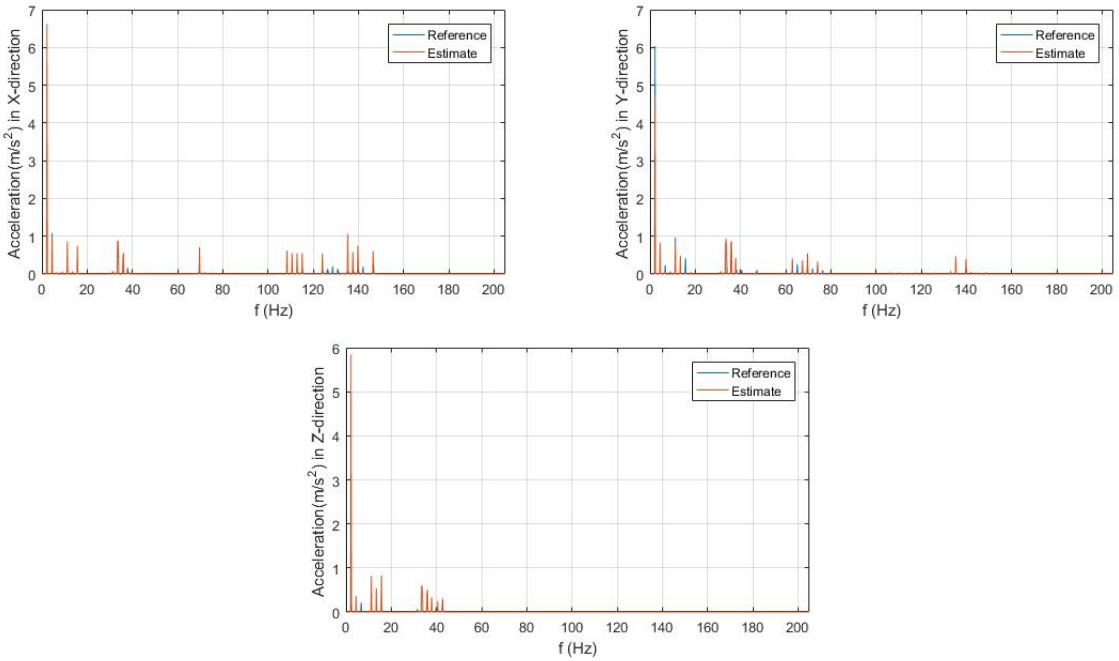

Figure 4.8: Comparison of reference and estimated acceleration profiles in X,Y and Z directions in frequency domain.

The same estimation procedure was conducted with motions of frequencies of 4.5 cycles per second and 8.5 cycles per second. The results obtained from all three motions are presented in Tables 4.1 and 4.2.

There might be multiple reasons for the errors in estimated peak values of the motion. One source of error might be the small angle assumption which was considered while constructing the rotation matrix at each time step. Also this assumption is followed by numerical integration of the angular velocity data, which might also be accountable for the error.

Table 4.1: Repeatability

Frequency (Hz)	**Distance moved along each axis (mm)**	**Repeatability(m/s^2)**		
		X-Axis	**Y-Axis**	**Z-axis**
2.3	90	1.42	0.78	0.38
4.5	20	0.51	0.66	0.30
8.5	7	1.42	1.73	0.95

Table 4.2: Error Analysis

Frequency (Hz)	**Added rotation (degrees)**	**RMS error (m/s^2)**		
		X-Axis	**Y-Axis**	**Z-axis**
2.3	25	1.67	1.19	0.42
4.5	8	0.69	1.13	0.36
8.5	5	1.59	2.26	1.28

Another source of error is the measurement of unwanted accelerations due to the rotational motion of the IMU. The cause for this is the improper alignment of the center of IMU and the center of the end effector about which the rotation takes place. It is practically impossible to eliminate this source of error, as it is difficult to find the center of rotation of the IMU. Since the combined motion of rotation and translation is carried out at the same frequencies, it becomes difficult for the filter to eliminate the effect of these unwanted acceleration components. However, in a real-world scenario, the rotational motion and translational motion might not be taking place at the same frequencies. In that case, the filter will not fail to remove the unwanted acceleration components. Due to the limitations of the robot, this type of scenario was not tested.

One way to eliminate the errors caused by the construction of rotation matrix is by employing a different method of representing the rotations. The small angle approximation was considered in this work to eliminate the need to know the exact order of rotation since multiplication of matrices does not obey the commutative law. However, when the rotations are represented using quarternions, the need to know the order of rotation is eliminated,

subsequently eliminating the small angle approximation. In [12] quaternions were used to represent the rotations experienced by the rigid body and the error between the estimates and the actual acceleration was small. Another way to get better estimation of the rotation matrix is by combing the gyroscope data and the data captured by the mangnetometer that is also present in the IMU by using sensor fusion techniques. For better noise removal, multi-level wavelet decomposition can be employed instead of using magnitude-based filtering.

CHAPTER 5

CONCLUSION

In this thesis, an algorithm to capture the acceleration profile of vibrations experienced by the driver of an off-road vehicle has been proposed. The inertial navigation algorithm in combination with a magnitude-based filter was used to obtain acceptable estimates of the global accelerations in three-dimensional space. The proposed algorithm was verified through experiments. The first experiment was conducted to check for the accuracy of the IMU in combination with the proposed algorithm in the absence of rotation. The estimated results show relatively small errors when compared to the reference signal. This indicates that the combined pair of IMU and the proposed algorithm performs with acceptable amount of accuracy.

The second experiment was conducted to evaluate the performance of the IMU in combination with the proposed algorithm in the presence of rotation. Even though the proposed algorithm is able to accurately estimate the overall profile of the global acceleration, the peak values of the estimated results had errors when compared with the reference profiles. Error analysis indicates that the proposed algorithm produces results at an acceptable degree of accuracy although further evaluation with actual field data is suggested.

The errors could be mainly attributed to two sources. The first source could be the small angle approximation used to contruct the rotation matrix at each time step followed by the numerical integration of the angular velocity data, and the second source of error could be the unwanted accelerations being measured by the IMU due to the misalignment between the IMU and the rotational axis.

REFERENCES

[1] Shadman Sakib. Implementation of digital IMU for increasing accuracy of hydrograpic survey. *Procedia Engineering*, 386–393. ELSEVIER, 2016.

[2] Guy Zaidner and Amir Shapiro. A novel data fusion algorithm for low-cost localization and navigation of autonomous vineyard sprayer robots. *Biosystems Engineering*,133–148, 2016.

[3] Jan Wendel, Oliver Meister, Christian Schlaile, and Gert F. Trommer. An integrated GPS/MEMS-IMU navigation system for an autonomous helicopter. *Aerospace Science and Technology*, 527–533. ELSEVIER, 2006.

[4] Lu Lou and Xu Xin. An approach to improve attitude estimation using sensor fusion for robot navigation. *Procedia Engineering*, 5601–5605. ELSEVIER, 2011.

[5] Wenchao Jiang and Zhaozheng Yin. Combining passive visual cameras and active IMU sensors for persistent pedestrian tracking *Journal of Visual Communication and Image Representation*. ELSEVIER, 2017.

[6] Vincenzo Ferrara, Andrea Pietrelli, Simone Chicarella, and Lara Pajewski. GPR/GPS/IMU system as buried objects locator. *Measurement*, 534–541. ELSEVIER, 2018.

[7] Zengke Li, Guobin Chang, Jingxiang Gao, Jian Wang, and Alberto Hernandez. GPS/UWB/MEMS-IMU tightly coupled navigation with improved robust Kalman filter. *Advances in Space Research*, 2424–2434. ELSEVIER, 2016.

[8] Yushuang Tian, Xiaoli Meng, Dapeng Tao, Dngquan Liu, and Chen Feng. Upper limb motion tracking with integration of IMU and kinect. *Neurocomputing*, 207–218. ELSEVIER, 2015.

[9] Hondge Dai, Jianhua Lu, Wei Guo, Guangbin Wu, and Xiaonan Wu. IMU-based deformation estimation about the deck of large ship. *Optik - International Journal for Light and Electron Optics*, 3535–3540. ELSEVIER, 2016.

[10] Song Lialiang, Zhang Xhunxi, and Chao Daihong. An elastic deformation measurement method for helicopter based on double-IMUs/DGPS TRAMS. *Measurements*, 1704–1714. ELSEVIER, 2013.

[11] Jan Karchnak, Dusan Simsik, Boris Jobbagy, Alena Galajdova, and Daniela Onofrejova. MEMS sensors in evaluation of human biomechanical parameters. *Procedia Engineering*, 209–215. ELSEVIER, 2014.

[12] Patrick Esser, Helen Dawes, Johnny Collett, and Ken Howells. IMU: Inertial Sensing of vertical COM mvement. *Journal of Biomechanics*,1578–1581. ELSEVIER, 2009.

[13] Jeong Ho Kim, Jack T. Dennerlein. and Peter W. Johnson. The effect of a multi-axis suspension on whole body vibration exposures and physical stress in the neck and low back in agricultural tractor applications *Applied Ergonomics*, 80–89. ELSEVIER, 2018

[14] Shaghayegh Zihajehzadeh, Darrell Loh, Tien Jung Lee, Reynald Hoskinson, and Edward J. Park. A cascaded Kalman filter-based GPS/MEMS-IMU integration for sports applications *Mearurement*. ELSEVIER, 2015.

[15] Marcus Schmidt, Carl Rheinlander, Kevin Frederic Nolte, Sebastin Wille, Norbert Wehn, and Thomas Jaitner. IMU-based determination of stance duration during sprinting. *Procedia Engineering*, 747–752. ELSEVIER, 2016

[16] Franklin Powell and Emami-Naina. *Feedback control of dynamic systems*. Pearson, 2015.

[17] Oliver J. Woodman. *An introduction to inertial navigation*. University of Cambridge, 2007.

[18] ADIS16405 Datasheet. *Analog Devices*.

[19] M.W. Spong, S. Hutchinson, and M. Vidyasagar. *Robot modelling and control*. 2004.

[20] Peter V. Oneil. *Advanced engineering mathematics*. Cengage Learning, 2012.

[21] John G. Proakis, and Dimitris G. Manolakis. *Digital signal processing*. Pearson,

2007.[22] Alan V. Oppenheim and Alan S. Willsky. *Signals and systems*. Pearson, 2014.